

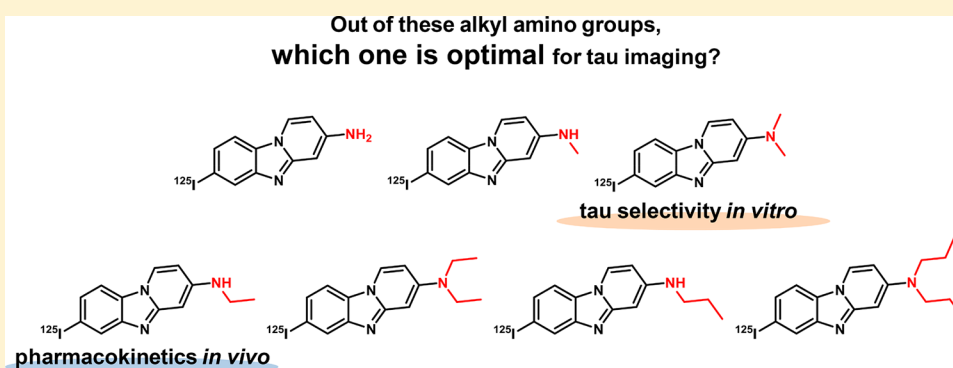
Structure–Activity Relationships of Radioiodinated Benzoimidazopyridine Derivatives for Detection of Tau Pathology

Sho Kaide,[†] Masahiro Ono,^{*,†,ⓑ} Hiroyuki Watanabe,[†] Ayane Kitada,[†] Masashi Yoshimura,[†] Yoichi Shimizu,[†] Masafumi Ihara,[‡] and Hideo Saji^{†,ⓑ}

[†]Department of Patho-Functional Bioanalysis, Graduate School of Pharmaceutical Sciences, Kyoto University, 46-29 Yoshida Shimoadachi-cho, Sakyo-ku, Kyoto 606-8501, Japan

[‡]Department of Stroke and Cerebrovascular Diseases, National Cerebral and Cardiovascular Center, 5-7-1 Fujishiro-dai, Suita, Osaka 565-8565, Japan

S Supporting Information



ABSTRACT: It is generally accepted that neurofibrillary tangles consisting of tau proteins are involved in the pathogenesis of Alzheimer's disease (AD). For selective detection of tau pathology, we synthesized and evaluated radioiodinated benzoimidazopyridine (BIP) derivatives with an alkylamino group as tau imaging probes. *In vitro* selectivity to tau aggregates and *in vivo* pharmacokinetics of BIP derivatives varied markedly, being strongly dependent on the alkylamino group. In *in vitro* autoradiography with AD brain sections, the BIP derivative with a dimethylamino group (BIP-NMe₂) showed the highest selectivity to tau aggregates. Regarding the biodistribution using normal mice, the BIP derivative with an ethylamino group (BIP-NHEt) showed the highest uptake (6.04% ID/g at 2 min postinjection) into and rapid washout (0.12% ID/g at 60 min postinjection) from the brain. These results suggest that the introduction of an optimal alkylamino group into the BIP scaffold may lead to the development of more potential tau imaging probes.

KEYWORDS: Alzheimer's disease (AD), radioiodinated benzoimidazopyridine (BIP), tau pathology, alkylamino group, alkyl chain, structure–activity relationships

Alzheimer's disease (AD), the most common cause of dementia, is a chronic neurodegenerative disorder characterized by memory loss, spatial disorientation, and cognitive impairment.¹ According to the World Alzheimer Report 2016, the global population has been growing rapidly, and it is a concern that more and more elderly people throughout the world will suffer from AD, necessitating the urgent development of imaging techniques for the early diagnosis and treatment of AD.² The typical neuropathological hallmarks in AD brains are senile plaques (SPs) and neurofibrillary tangles (NFTs), which are formed by amyloid β peptides ($A\beta$) and hyperphosphorylated tau aggregates, respectively.³ Those abnormal deposits are known to be principal biomarkers in AD brains, and they are major targets of both basic and clinical studies of AD. In the past, various $A\beta$ imaging studies were developed in order to diagnose AD at an early stage;⁴ however, a lot of recent $A\beta$ imaging studies in

clinical stages show that there are numerous false-positive subjects who show the deposition of $A\beta$ plaques in the brain but do not have AD.⁵

It is well-known that the accumulation of tau proteins correlates with clinical conditions of AD more precisely than that of $A\beta$ plaques, and it is considered to be a more important and attractive imaging target for the diagnosis and treatment of AD.⁶ From these clinical viewpoints, a series of first-generation tau-selective imaging tracers for positron emission tomography (PET) such as [¹¹C]PBB3, [¹⁸F]AV1451 (flortaucipir or T807), and [¹⁸F]THK5351 has recently been developed and energetically studied regarding the utility in clinical stages.^{7–9} Despite several promising clinical data on these tau PET tracers, the

Received: February 22, 2018

Accepted: March 29, 2018

limitation of the number of facilities for PET throughout the world and the relatively short half-life of radionuclides for PET are disadvantages, which restrict its use. In addition, recent studies reported that some tau PET tracers displayed nonspecific accumulation in subcortical white matter or high “off-target” binding; in other words, tracer retention occurs in brain areas considered not to have tau deposits, such as the choroid plexus, basal ganglia, and midbrain.¹⁰ This is a crucial problem in the development of first-generation tau tracers. Second-generation tau radiotracers for PET including [¹⁸F]-RO6958948, [¹⁸F]-MK6240, and [¹⁸F]-PI2620, which are less or not affected by “off-target” binding, have recently been reported.^{11–13}

Single photon emission computed tomography (SPECT) is known as another nuclear medical modality capable of the invasive imaging of a living body as well as PET. Since there are numerous facilities for SPECT throughout the world and the half-life of radionuclides used for SPECT is relatively long, it is generally accepted that SPECT is the convenient imaging modality for preclinical and clinical use. Nevertheless, most tau tracers under clinical studies are for PET¹⁴ and no clinically useful SPECT tracer has been reported.^{15–17}

Over the past few years, we have developed original tau SPECT tracers with a radioiodinated benzoimidazopyridine (BIP) scaffold and studied their structure–activity relationships (SARs) by the introduction of various kinds of groups into a BIP scaffold (Figure 1).¹⁸ The BIP derivative with a

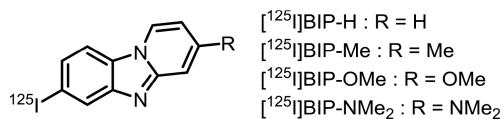


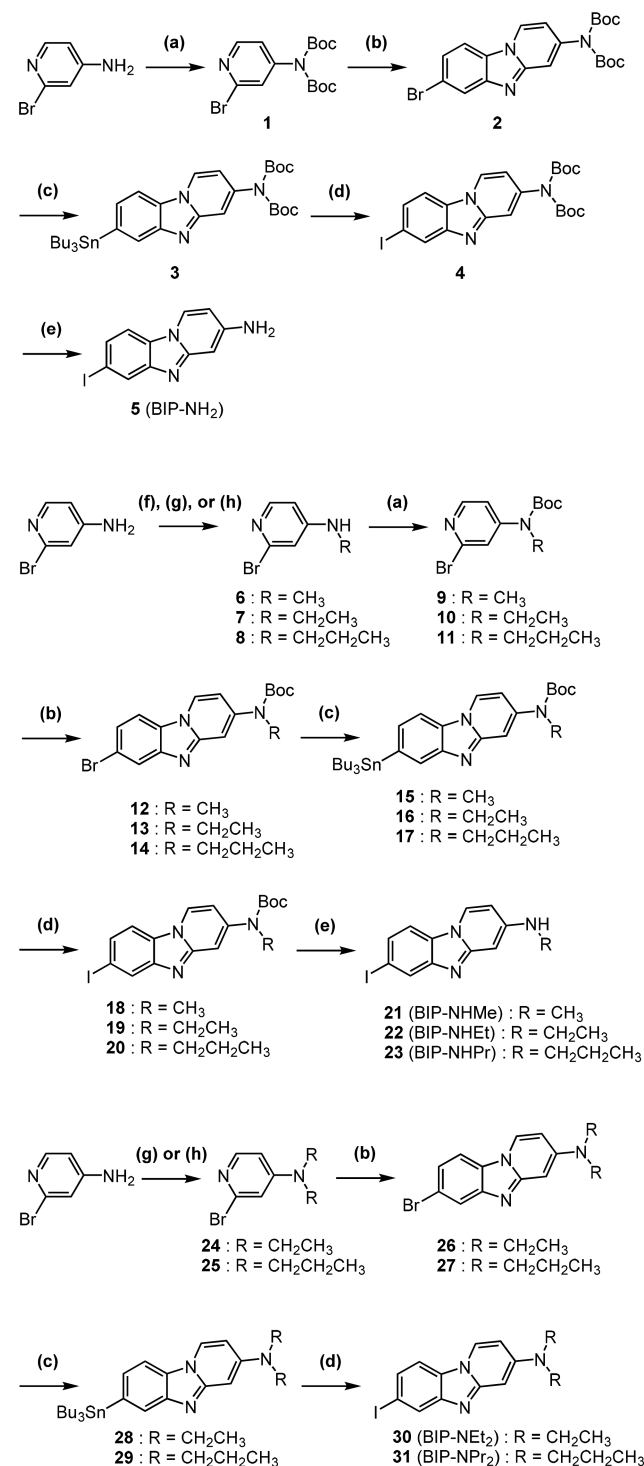
Figure 1. ¹²⁵I-labeled BIP derivatives reported as tau imaging probes.

dimethylamino group (BIP-NMe₂) most notably displayed high *in vitro* selective affinity for tau aggregates against Aβ plaques and preferable *in vivo* pharmacokinetics in the brain of normal mice as compared to other BIP derivatives with a methyl and methoxy group.¹⁸ Some tau PET radiotracers including [¹¹C]-PBB3 and [¹⁸F]-THK5351 also have an alkylamino group. These findings suggested that an alkylamino group with a BIP scaffold might have beneficial effects on the characteristics as a tau targeting probe.

In this study, we designed and synthesized novel six radioiodinated BIP derivatives with amino, methylamino, ethylamino, diethylamino, propylamino, and dipropylamino groups (abbreviated as BIP-NH₂, BIP-NHMe, BIP-NHEt, BIP-NEt₂, BIP-NHPr, and BIP-NPr₂, respectively) in order to evaluate how the alkyl chain on the amino group introduced into the 3-position of the BIP scaffold affects the *in vitro* selectivity to tau aggregates and *in vivo* pharmacokinetics in the brain. Here, we report a SAR study of radioiodinated BIP derivatives as tau imaging probes.

We synthesized BIP derivatives according to Scheme 1. 2-Bromopyridine derivatives (**1**, **9**, **10**, **11**, **24**, and **25**) for BIP-NH₂, BIP-NHMe, BIP-NHEt, BIP-NHPr, BIP-NEt₂, and BIP-NPr₂ were synthesized by alkylation and introduction of the protecting group on the amino group of 4-amino-2-bromopyridine. The formation of the BIP scaffold was achieved by the reaction of 2-bromopyridine derivatives with 2,5-dibromoaniline, 1,10-phenanthroline, and cesium carbonate by following the method reported previously¹⁹ to obtain bromo

Scheme 1^a

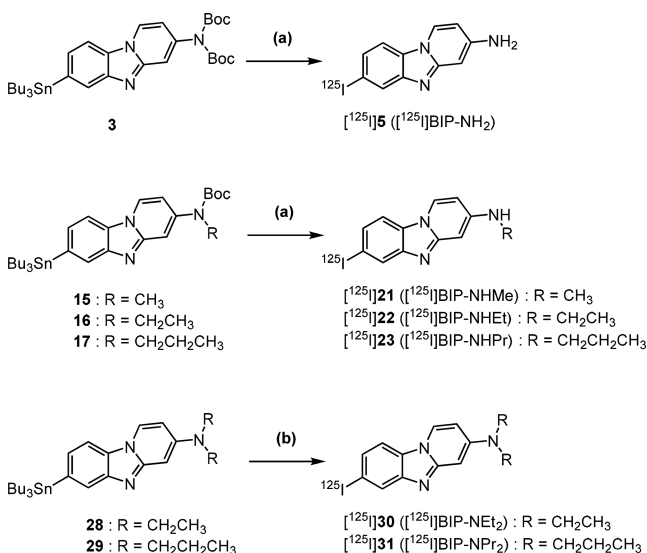


^aReagent and conditions: (a) Boc₂O, DMAP, Et₃N, THF, 80 °C; (b) 2,5-dibromoaniline, CuI(I), 1,10-phenanthroline, Cs₂CO₃, xylene, 120 °C; (c) (SnBu₃)₃, Pd(PPh₃)₄, Et₃N, dioxane, 95 °C; (d) I₂, CHCl₃, rt; (e) TFA, CH₂Cl₂, rt; (f) CH₃I, NaH, 0 °C; (g) CH₃CH₂I, NaH, 0 °C; (h) CH₃CH₂CH₂I, NaH, 0 °C.

compounds (**2**, **12**, **13**, **14**, **26**, and **27**). Thereafter, the tributyltin derivatives (**3**, **15**, **16**, **17**, **28**, and **29**) were prepared from the corresponding bromo compounds in the presence of catalyst, Pd(0). The iodo compounds (**4**, **18**, **19**, **20**, **30**, and **31**) were obtained from the tributyltin derivatives by the

reaction with I_2 in chloroform at room temperature. The final compounds with amino or mono alkyl amino group (**5**, **21**, **22**, and **23**) were obtained through removing the protecting group by trifluoroacetic acid.

In this study, ^{125}I was used as a radioiodine instead of ^{123}I as it is readily available and has longer half-life. ^{125}I -labeled BIP derivatives were obtained from the corresponding tributyltin derivatives by the iododestannylation reaction with the oxidant, hydrogen peroxide (Scheme 2). Radiochemical yields of ^{125}I -labeling reaction were 25.1–64.6%, and radiochemical purities were over 95% after purification using HPLC.

Scheme 2^a

^aReagent and conditions: (a) (1) ^{125}I]NaI, H₂O₂, 1 N HCl, rt; (2) TFA, CHCl₃; (b) ^{125}I]NaI, H₂O₂, 1 N HCl, rt.

In order to evaluate selective binding affinity for tau aggregates against A β plaques, we carried out *in vitro* autoradiography (ARG) using AD brain sections. Before this experiment, we conducted immunohistochemical staining of AD brain sections from frontal and temporal lobes with anti-A β antibody and antiphosphorylated tau antibody according to the method reported previously (Figure S1).²⁰ Desirable tau tracers should selectively accumulate only in the gray matter of the temporal lobe without marked accumulation in the gray matter of the frontal lobe, which is the tau accumulation pattern in immunohistochemical staining.

The *in vitro* autoradiograms of ^{125}I]BIP-NMe₂ and novel ^{125}I]BIP derivatives are shown in Figure 2. When optimal adjustment of the autoradiograms for each probe was performed, almost all ^{125}I]BIP derivatives (^{125}I]BIP-NH₂, ^{125}I]BIP-NHMe, ^{125}I]BIP-NMe₂, ^{125}I]BIP-NHEt, ^{125}I]BIP-NEt₂, and ^{125}I]BIP-NHPr) markedly accumulated in the gray matter of the temporal lobe, suggesting that these novel BIP derivatives with the alkylamino group selectively bound to tau aggregates, similarly to ^{125}I]BIP-NMe₂.¹⁸ Conversely, these BIP derivatives did not markedly accumulate at all in the gray matter of the frontal lobe. Surprisingly, ^{125}I]BIP-NPr₂ accumulated in neither the gray matter of the frontal lobe nor the gray matter of the temporal lobe, mainly owing to the lipophilicity of ^{125}I]BIP-NPr₂, which resulted in relatively high nonspecific accumulation in the white matter of the frontal and temporal lobes.

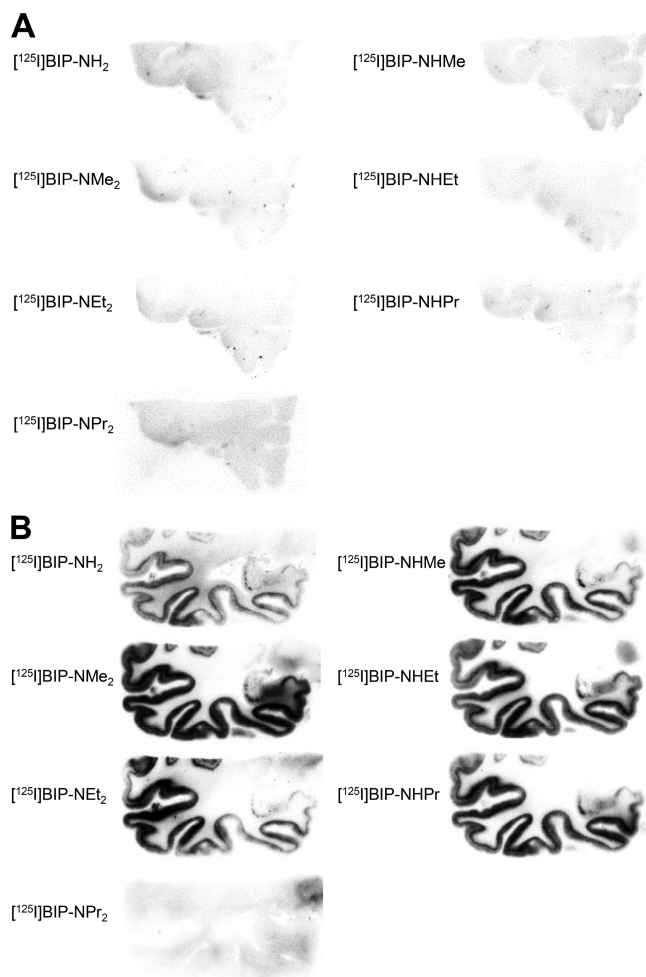


Figure 2. Comparison of *in vitro* autoradiograms with ^{125}I -labeled BIP derivatives in AD brain sections from the frontal (A) and temporal (B) lobes.

Then, we compared a high-magnification image of an *in vitro* autoradiogram of ^{125}I]BIP-NHMe with that of immunohistochemical staining (Figure S1). Radioactivity accumulation of ^{125}I]BIP-NHMe (Figure S1A) was laminar along the gray matter of the temporal lobe, which is characteristic of tau accumulation stained with antiphosphorylated tau antibody (Figure S1B) and did not match with the pattern of A β accumulation stained with anti-A β antibody (Figure S1C). The coincidence of the radioactivity accumulation pattern with immunohistochemical staining confirmed that ^{125}I]BIP-NH₂, ^{125}I]BIP-NHMe, ^{125}I]BIP-NHEt, ^{125}I]BIP-NEt₂, and ^{125}I]BIP-NHPr selectively recognized tau aggregates, indicating that they may detect tau pathology in AD brains.

Thereafter, the quantitative analysis of the *in vitro* autoradiograms mentioned above was performed. We set four areas in AD brain sections (the gray matter of the frontal lobe, white matter of the frontal lobe, gray matter of the temporal lobe, and white matter of the temporal lobe) as the regions of interest (ROIs) and analyzed the accumulation of the radioactivity (counts per minute per square millimeter, abbreviated as cpm/mm²) for each ROI and each probe ($n = 3-4$) (Figure 3). Then, the selectivity of binding to tau aggregates against A β plaques was evaluated by calculating the ratio of the radioactivity accumulation in the gray matter of the temporal lobe (A β plaques (+), tau aggregates (+)) against the gray

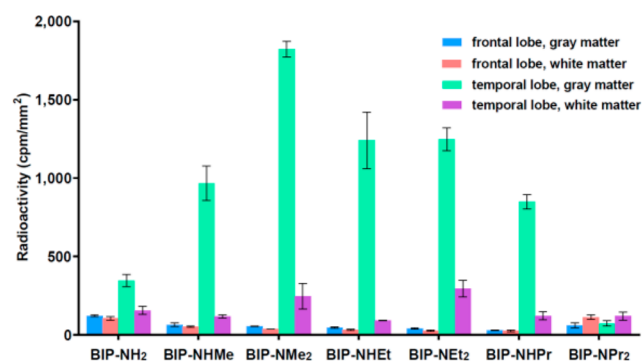


Figure 3. Quantitative analysis of *in vitro* autoradiography with AD brain sections. Data are presented as the mean \pm SEM ($n = 3-4$).

matter of the frontal lobe ($A\beta$ plaques (+), tau aggregates (-)) (Table 1).

Table 1. Ratio of Radioactivity Accumulation in the Gray Matter of the Temporal Lobe (a) against the Gray Matter of the Frontal Lobe (b)

compd	a/b ratio
[¹²⁵ I]BIP-NH ₂	2.9
[¹²⁵ I]BIP-NHMe	14.7
[¹²⁵ I]BIP-NMe ₂	32.8
[¹²⁵ I]BIP-NHEt	26.2
[¹²⁵ I]BIP-NEt ₂	30.5
[¹²⁵ I]BIP-NHPr	29.2
[¹²⁵ I]BIP-NPr ₂	1.2

Compared with [¹²⁵I]BIP-NMe₂ (32.8), reported as a highly selective tau imaging probe,¹⁸ [¹²⁵I]BIP-NHEt, [¹²⁵I]BIP-NEt₂, and [¹²⁵I]BIP-NHPr showed high ratios (26.2, 30.5, and 29.2, respectively) at the same level, meaning that they may function as tau-selective imaging probes. [¹²⁵I]BIP-NPr₂ displayed a very low ratio (1.2) because [¹²⁵I]BIP-NPr₂ accumulated evenly in the gray matter of the temporal and frontal lobes, which demonstrated that [¹²⁵I]BIP-NPr₂ did not show selectivity to tau aggregates at all. Although a wide variation in the ratio of each [¹²⁵I]BIP derivative (1.2–32.8) was observed, the dimethylamino group had the most favorable effect on *in vitro* tau selectivity among all alkylamino groups used in this study.

To evaluate the radioactivity pharmacokinetics after the injection of BIP derivatives into normal mice, we performed a biodistribution study with each compound (Figure 4 and Table 2). In order to specifically detect tau aggregates in the brain, preferable probes targeting tau aggregates are desired to be highly taken at an early time point after injection and rapidly washed out from the brain because normal mice have no tau deposits in the brain.²¹ The radioactivity accumulation of [¹²⁵I]BIP derivatives in the brain was 2.01–6.04 percentage injected dose per gram (% ID/g) at 2 min postinjection. Thereafter, it was dispersed with time, decreasing to 0.38–0.66% ID/g and 0.12–0.28% ID/g at 30 and 60 min postinjection, respectively.

In order to evaluate the utility as a tau imaging probe, the initial brain uptake of each [¹²⁵I]BIP derivative was compared. Highly hydrophilic [¹²⁵I]BIP-NH₂ and highly lipophilic [¹²⁵I]BIP-NPr₂ exhibited lower initial brain uptakes (2.01 and 2.79% ID/g at 2 min postinjection, respectively) than [¹²⁵I]BIP-

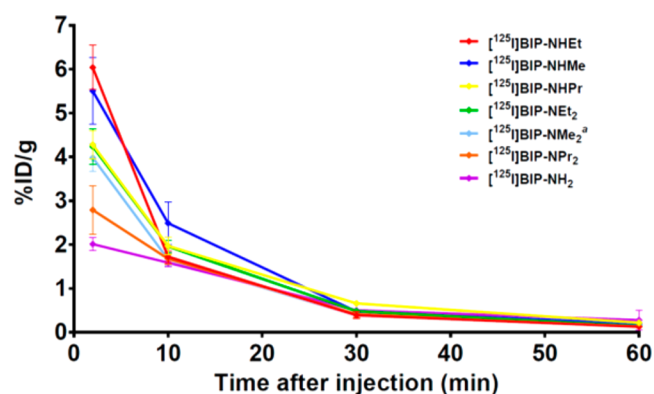


Figure 4. Comparison of uptake into and clearance from the brain after the intravenous injection of ¹²⁵I-labeled BIP derivatives into normal mice ($n = 5$). ^aData were reported previously.¹⁸

NMe₂ (3.98% ID/g),¹⁸ revealing that in comparison of [¹²⁵I]BIP-NMe₂ (log P-value = 2.40 ± 0.05),¹⁸ [¹²⁵I]BIP-NH₂ may be too hydrophilic (log P-value = 2.08 ± 0.01) and [¹²⁵I]BIP-NPr₂ may be too lipophilic (log P-value = 3.40 ± 0.02) to sufficiently penetrate the blood–brain barrier (BBB) of mice at an initial time point. Conversely, among [¹²⁵I]BIP derivatives with an alkylamino group, [¹²⁵I]BIP-NHMe and [¹²⁵I]BIP-NHEt showed notably higher brain uptakes at 2 min postinjection (5.51 and 6.04% ID/g, respectively) than [¹²⁵I]BIP-NMe₂, due to the moderate lipophilicity and a molecular size permitting optimal passive brain uptake *in vivo*. Moreover, they showed higher initial brain uptakes than [¹¹C]PBB3,²² [¹⁸F]T807,⁸ and [¹⁸F]THK5351⁹ reported previously as tau imaging tracers undergoing clinical research (1.92, 4.43, and 4.35% ID/g, respectively). In addition, the brain uptake of [¹²⁵I]BIP-NHMe, [¹²⁵I]BIP-NHEt, and [¹²⁵I]BIP-NHPr at 2 min postinjection was higher than that of [¹²⁵I]BIP-NMe₂, [¹²⁵I]BIP-NEt₂, and [¹²⁵I]BIP-NPr₂, respectively, which suggested that BIP derivatives with a monoalkylamino group penetrated the BBB more easily than the corresponding BIP derivatives with a dialkylamino group. These results were consistent with previous reports that the lipophilicity and molecular size of a compound affect its ability to permeate the brain.^{20,23}

Then, clearance from the brain was evaluated by calculating the ratio of radioactivity accumulation. The values were 4.0–15.5 for 2 min/30 min and 7.2–47.2 for 2 min/60 min, respectively. [¹²⁵I]BIP-NHMe and [¹²⁵I]BIP-NHEt displayed higher 2 min/60 min ratios (28.5 and 47.2, respectively) than [¹²⁵I]BIP-NMe₂ (24.9)¹⁸ and 2 min/30 min ratios (11.6 and 15.5, respectively) as high as [¹¹C]PBB3,⁷ [¹⁸F]T807,⁸ and [¹⁸F]THK5351⁹ (17.5, 20.7, and 7.15 for the initial time point/30 min, respectively), indicating that they showed rapid washout from the brain due to their low nonspecific binding. These findings suggest that [¹²⁵I]BIP-NHMe and [¹²⁵I]BIP-NHEt may meet the standards of the pharmacokinetics in the brain for clinical evaluations.^{24,25}

[¹²⁵I]BIP-NHMe and [¹²⁵I]BIP-NHEt accumulated initially in the liver (liver_{2 min} = 9.9 and 13.5% ID/g, respectively) and subsequently in the intestine (intestine_{60 min} = 27.6 and 21.3% ID/g, respectively) (Table S1) as well as other [¹²⁵I]BIP derivatives, which may be attributable to their lipophilicity. It was reported that the lipophilic compounds showed similar accumulation patterns to [¹²⁵I]BIP derivatives in mice.¹⁸ Their accumulations in the thyroid were negligible (thyroid_{60 min} =

Table 2. Brain Uptake of Radioactivity after the Injection of Each ¹²⁵I-Labeled BIP Derivative in Normal Mice^a and the Ratio of Their Radioactivity Accumulation (2 min/30 and 2 min/60 min)

compd	%ID/g in the brain			ratio	
	2 min	30 min	60 min	2 min/30 min	2 min/60 min
[¹²⁵ I]BIP-NH ₂	2.01 (0.15)	0.50 (0.07)	0.28 (0.23)	4.0	7.2
[¹²⁵ I]BIP-NHMe	5.51 (0.77)	0.47 (0.03)	0.19 (0.02)	11.6	28.5
[¹²⁵ I]BIP-NMe ₂ ^b	3.98 (0.32)	0.38 (0.03)	0.16 (0.01)	10.5	24.9
[¹²⁵ I]BIP-NHEt	6.04 (0.51)	0.39 (0.08)	0.12 (0.02)	15.5	47.2
[¹²⁵ I]BIP-NEt ₂	4.23 (0.41)	0.48 (0.04)	0.14 (0.03)	8.8	30.3
[¹²⁵ I]BIP-NHPr	4.28 (0.33)	0.66 (0.05)	0.21 (0.04)	6.5	20.4
[¹²⁵ I]BIP-NPr ₂	2.79 (0.55)	0.41 (0.08)	0.12 (0.04)	6.8	22.0

^aEach value represents the mean (SD) of five animals. ^bThe data were reported previously.¹⁸

0.08 and 0.30% ID, respectively), indicating that they may remain stable toward deiodination *in vivo* until 60 min postinjection. On the basis of the biodistribution experiment with normal mice, it was clarified that the ethylamino group, in particular, contributed to preferable *in vivo* pharmacokinetics in the brain.

In conclusion, this study revealed for the first time that the alkyl chain on the amino group introduced into the 3-position of the BIP scaffold has a critically important impact on the *in vitro* binding selectivity to tau aggregates and *in vivo* pharmacokinetics. Among alkylamino groups evaluated in the present study, the dimethylamino and ethylamino groups had beneficial effects on *in vitro* tau selectivity and *in vivo* uptake into and washout from the brain, respectively, based on the radioiodinated BIP scaffold. These results suggest that a radioiodinated BIP derivative with an ideal alkylamino group may function as a potentially useful SPECT probe for imaging tau aggregates in the brain.

■ ASSOCIATED CONTENT

● Supporting Information

The Supporting Information is available free of charge on the ACS Publications website at DOI: [10.1021/acsmchemlett.8b00092](https://doi.org/10.1021/acsmchemlett.8b00092).

Results of immunohistochemical staining, high magnification of an *in vitro* autoradiogram with [¹²⁵I]BIP-NHMe and immunohistochemical staining, the biodistribution study for all organs, procedures for the preparation of nonradiolabeled BIP derivatives (BIP-NH₂, BIP-NHMe, BIP-NHEt, BIP-NEt₂, BIP-NHPr, and BIP-NPr₂) and radioiodinated BIP derivatives ([¹²⁵I]BIP-NH₂, [¹²⁵I]BIP-NHMe, [¹²⁵I]BIP-NHEt, [¹²⁵I]BIP-NEt₂, [¹²⁵I]BIP-NHPr, and [¹²⁵I]BIP-NPr₂), immunohistochemical staining, *in vitro* autoradiography with AD brain sections, *in vivo* biodistribution study in normal mice, and measurement of log P-values (PDF)

■ AUTHOR INFORMATION

Corresponding Author

*Tel: +81-75-753-4608. Fax: +81-75-753-4568. E-mail: ono@pharm.kyoto-u.ac.jp.

ORCID

Masahiro Ono: [0000-0002-2497-039X](https://orcid.org/0000-0002-2497-039X)

Hideo Saji: [0000-0002-3077-9321](https://orcid.org/0000-0002-3077-9321)

Funding

This research was supported by JSPS KAKENHI Grant Numbers JP15H01555, JP17H04260, JP17H05092, and

JP17H05694, AMED under Grant Number JP16lm0103006j0005, and Japan Research Foundation for Clinical Pharmacology.

Notes

The authors declare no competing financial interest.

■ ABBREVIATIONS

Aβ, amyloid β; AD, Alzheimer's disease; SP, senile plaque; NFT, neurofibrillary tangle; PET, positron emission tomography; SPECT, single photon emission computed tomography; BIP, benzoimidazopyridine; SAR, structure–activity relationship; ARG, autoradiography; cpm, counts per minute; % ID/g, percentage injected dose per gram; BBB, blood–brain barrier; HPLC, high-performance liquid chromatography; Boc, *tert*-butoxycarbonyl; DMAP, *N,N*-dimethyl-4-aminopyridine; Et₃N, triethylamine; THF, tetrahydrofuran; TFA, trifluoroacetic acid; DMF, *N,N*-dimethylformamide

■ REFERENCES

- (1) Citron, M. Alzheimer's disease: strategies for disease modification. *Nat. Rev. Drug Discovery* **2010**, *9*, 387–398.
- (2) Du, X.; Wang, X.; Geng, M. Alzheimer's disease hypothesis and related therapies. *Transl. Neurodegener.* **2018**, *7*, 2.
- (3) Serrano-Pozo, A.; Frosch, M. P.; Masliah, E.; Hyman, B. T. Neuropathological alterations in Alzheimer disease. *Cold Spring Harbor Perspect. Med.* **2011**, *1*, a006189.
- (4) Svedberg, M. M.; Rahman, O.; Hall, H. Preclinical studies of potential amyloid binding PET/SPECT ligands in Alzheimer's disease. *Nucl. Med. Biol.* **2012**, *39*, 484–501.
- (5) Rowe, C. C.; Ng, S.; Ackermann, U.; Gong, S. J.; Pike, K.; Savage, G.; Cowie, T. F.; Dickinson, K. L.; Maruff, P.; Darby, D.; Smith, C.; Woodward, M.; Merory, J.; Tochon-Danguy, H.; O'Keefe, G.; Klunk, W. E.; Mathis, C. A.; Price, J. C.; Masters, C. L.; Villemagne, V. L. Imaging β-amyloid burden in aging and dementia. *Neurology* **2007**, *68*, 1718–1725.
- (6) Villemagne, V. L.; Fodero-Tavoletti, M. T.; Masters, C. L.; Rowe, C. C. Tau imaging: early progress and future directions. *Lancet Neurol.* **2015**, *14*, 114–124.
- (7) Maruyama, M.; Shimada, H.; Sahara, T.; Shinotoh, H.; Ji, B.; Maeda, J.; Zhang, M. R.; Trojanowski, J. Q.; Lee, V. M.; Ono, M.; Masamoto, K.; Takano, H.; Sahara, N.; Iwata, N.; Okamura, N.; Furumoto, S.; Kudo, Y.; Chang, Q.; Saido, T. C.; Takashima, A.; Lewis, J.; Jang, M. K.; Aoki, I.; Ito, H.; Higuchi, M. Imaging of tau pathology in a tauopathy mouse model and in Alzheimer patients compared to normal controls. *Neuron* **2013**, *79*, 1094–1108.
- (8) Xia, C. F.; Arteaga, J.; Chen, G.; Gangadharmath, U.; Gomez, L. F.; Kasi, D.; Lam, C.; Liang, Q.; Liu, C.; Mocharla, V. P.; Mu, F.; Sinha, A.; Su, H.; Szardenings, A. K.; Walsh, J. C.; Wang, E.; Yu, C.; Zhang, W.; Zhao, T.; Kolb, H. C. [¹⁸F]T807, a novel tau positron emission tomography imaging agent for Alzheimer's disease. *Alzheimer's Dementia* **2013**, *9*, 666–676.

- (9) Harada, R.; Okamura, N.; Furumoto, S.; Furukawa, K.; Ishiki, A.; Tomita, N.; Tago, T.; Hiraoka, K.; Watanuki, S.; Shidahara, M.; Miyake, M.; Ishikawa, Y.; Matsuda, R.; Inami, A.; Yoshikawa, T.; Funaki, Y.; Iwata, R.; Tashiro, M.; Yanai, K.; Arai, H.; Kudo, Y. ¹⁸F-THK5351: A Novel PET Radiotracer for Imaging Neurofibrillary Pathology in Alzheimer Disease. *J. Nucl. Med.* **2016**, *57*, 208–214.
- (10) Villemagne, V. L. Selective Tau Imaging: Der Stand der Dinge. *J. Nucl. Med.* **2018**, *59*, 175–176.
- (11) Gobbi, L. C.; Knust, H.; Korner, M.; Honer, M.; Czech, C.; Belli, S.; Muri, D.; Edelmann, M. R.; Hartung, T.; Erbsmehl, I.; Grall-Ulsemmer, S.; Koblet, A.; Rueher, M.; Steiner, S.; Ravert, H. T.; Mathews, W. B.; Holt, D. P.; Kuwabara, H.; Valentine, H.; Dannals, R. F.; Wong, D. F.; Borroni, E. Identification of Three Novel Radiotracers for Imaging Aggregated Tau in Alzheimer's Disease with Positron Emission Tomography. *J. Med. Chem.* **2017**, *60*, 7350–7370.
- (12) Walji, A. M.; Hostetler, E. D.; Selnick, H.; Zeng, Z.; Miller, P.; Bennacef, I.; Salinas, C.; Connolly, B.; Gantert, L.; Holahan, M.; O'Malley, S.; Purcell, M.; Riffel, K.; Li, J.; Balsells, J.; O'Brien, J. A.; Melquist, S.; Soriano, A.; Zhang, X.; Ogawa, A.; Xu, S.; Joshi, E.; Della Rocca, J.; Hess, F. J.; Schachter, J.; Hesk, D.; Schenk, D.; Struyk, A.; Babaoglu, K.; Lohith, T. G.; Wang, Y.; Yang, K.; Fu, J.; Evelhoch, J. L.; Coleman, P. J. Discovery of 6-(Fluoro-¹⁸F)-3-(1H-pyrrolo[2,3-c]-pyridin-1-yl)isoquinolin-5-amine ([¹⁸F]-MK-6240): A Positron Emission Tomography (PET) Imaging Agent for Quantification of Neurofibrillary Tangles (NFTs). *J. Med. Chem.* **2016**, *59*, 4778–4789.
- (13) Mueller, A.; Kroth, H.; Berndt, M.; Capotosti, F.; Molette, J.; Schieferstein, H.; Oden, F.; Juergens, T.; Darmency, V.; Schmitt-Willich, H.; Hickman, D.; Tamagnan, G.; Pfeifer, A.; Dinkelborg, L.; Stephens, A.; Muhs, A. Characterization of the novel PET Tracer PI-2620 for the assessment of Tau pathology in Alzheimer's disease and other tauopathies. *J. Nucl. Med.* **2017**, *58*, 847.
- (14) Saint-Aubert, L.; Lemoine, L.; Chiotis, K.; Leuzy, A.; Rodriguez-Vieitez, E.; Nordberg, A. Tau PET imaging: present and future directions. *Mol. Neurodegener.* **2017**, *12*, 19.
- (15) Ono, M.; Hayashi, S.; Matsumura, K.; Kimura, H.; Okamoto, Y.; Ihara, M.; Takahashi, R.; Mori, H.; Saji, H. Rhodanine and thiohydantoin derivatives for detecting tau pathology in Alzheimer's brains. *ACS Chem. Neurosci.* **2011**, *2*, 269–275.
- (16) Matsumura, K.; Ono, M.; Hayashi, S.; Kimura, H.; Okamoto, Y.; Ihara, M.; Takahashi, R.; Mori, H.; Saji, H. Phenylidiazanyl benzothiazole derivatives as probes for in vivo imaging of neurofibrillary tangles in Alzheimer's disease brains. *MedChemComm* **2011**, *2*, 596–600.
- (17) Watanabe, H.; Ono, M.; Kimura, H.; Matsumura, K.; Yoshimura, M.; Okamoto, Y.; Ihara, M.; Takahashi, R.; Saji, H. Synthesis and biological evaluation of novel oxindole derivatives for imaging neurofibrillary tangles in Alzheimer's disease. *Bioorg. Med. Chem. Lett.* **2012**, *22*, 5700–5703.
- (18) Ono, M.; Watanabe, H.; Kitada, A.; Matsumura, K.; Ihara, M.; Saji, H. Highly Selective Tau-SPECT Imaging Probes for Detection of Neurofibrillary Tangles in Alzheimer's Disease. *Sci. Rep.* **2016**, *6*, 34197.
- (19) Wu, Z.; Huang, Q.; Zhou, X.; Yu, L.; Li, Z.; Wu, D. Synthesis of Pyrido[1,2-a]benzimidazoles through a Copper-Catalyzed Cascade C-N Coupling Process. *Eur. J. Org. Chem.* **2011**, *2011*, 5242–5245.
- (20) Matsumura, K.; Ono, M.; Kitada, A.; Watanabe, H.; Yoshimura, M.; Iikuni, S.; Kimura, H.; Okamoto, Y.; Ihara, M.; Saji, H. Structure-Activity Relationship Study of Heterocyclic Phenylethenyl and Pyridinylethenyl Derivatives as Tau-Imaging Agents That Selectively Detect Neurofibrillary Tangles in Alzheimer's Disease Brains. *J. Med. Chem.* **2015**, *58*, 7241–7257.
- (21) Ono, M.; Saji, H. SPECT Imaging Agents for Detecting Cerebral β -Amyloid Plaques. *Int. J. Mol. Imaging* **2011**, *2011*, 543267.
- (22) Hashimoto, H.; Kawamura, K.; Igarashi, N.; Takei, M.; Fujishiro, T.; Aihara, Y.; Shiomi, S.; Muto, M.; Ito, T.; Furutsuka, K.; Yamasaki, T.; Yui, J.; Xie, L.; Ono, M.; Hatori, A.; Nemoto, K.; Sahara, T.; Higuchi, M.; Zhang, M. R. Radiosynthesis, photoisomerization, biodistribution, and metabolite analysis of ¹¹C-PBB3 as a clinically useful PET probe for imaging of tau pathology. *J. Nucl. Med.* **2014**, *55*, 1532–1538.
- (23) Zhuang, Z. P.; Kung, M. P.; Wilson, A.; Lee, C. W.; Plossl, K.; Hou, C.; Holtzman, D. M.; Kung, H. F. Structure-activity relationship of imidazo[1,2-a]pyridines as ligands for detecting β -amyloid plaques in the brain. *J. Med. Chem.* **2003**, *46*, 237–243.
- (24) Okamura, N.; Harada, R.; Furumoto, S.; Arai, H.; Yanai, K.; Kudo, Y. Tau PET imaging in Alzheimer's disease. *Curr. Neurol. Neurosci. Rep.* **2014**, *14*, 500.
- (25) Mason, N. S.; Mathis, C. A.; Klunk, W. E. Positron emission tomography radioligands for in vivo imaging of A β plaques. *J. Labelled Compd. Radiopharm.* **2013**, *56*, 89–95.